Chemical Thermodynamics and Thermal Analysis 18 (2025) 100170

Contents lists available at ScienceDirect

Chemical Thermodynamics and Thermal Analysis

journal homepage: www.elsevier.com/locate/ctta

Heat capacity of ethylene carbonate and ethyl methyl carbonate for the liquid phase at elevated temperatures

Philipp Finster *, Judith Jung, Magnus Rohde, Hans Jürgen Seifert, Carlos Ziebert

Karlsruhe Institute of Technology (KIT), Institute for Applied Materials - Applied Materials Physics (IAM-AWP), Hermann-von-Helmholtz-Platz 1, Eggenstein-Leopoldshafen, 76344, Germany

ARTICLE INFO

Keywords:
Lithium-ion battery
Heat capacity
Differential scanning calorimetry
Ethylene carbonate
Ethyl methyl carbonate

ABSTRACT

The heat capacities of liquid ethylene carbonate (EC) and ethyl methyl carbonate (EMC), two important electrolyte components for capacitors and Lithium-ion-batteries, were measured using differential scanning calorimetry in the temperature range from 263 to 500 K in heating mode and from 493 to 273 K in cooling mode for EC. The effect of the supercooled liquid of EC on the heat capacity is discussed. The heat capacity of EMC was determined from 211 to 360 K in heating mode. Based on the obtained heat capacities and the literature data, a simplified Maier–Kelley-fit for the heat capacities is provided. The temperature range of the experimentally determined heat capacity of the liquid state was extended to higher temperatures than previously reported in literature.

1. Introduction

Ethylene carbonate (EC) and ethyl methyl carbonate (EMC) are two extensively used and examined carbonates. They are used as solvents, for example in pharmaceutical production or in paints. Another application is the electrochemical field. Here the two carbonates are used as solvents in the electrolyte of capacitors and Lithium-ion-batteries (LIB). For those applications and their regular use cases, the temperature range is between 250 and 350 K. In this temperature range, sufficient thermodynamic data, such as heat capacity, are described by the literature.

More recently new processes arise, like the proposed synthesis of dimethyl carbonate from a mixture of EC and methanol at a temperature of about 433 K by Kim et al. [1] or the polymerization of EC also at 433 K by Lee and Litt [2]. Consequently, there is a need for heat capacity data at higher temperatures than 350 K. In the electrochemical field there is also a need for higher temperature data, due to the rising use of LIB. Here the practical demand is focussed on irregular scenarios, like the overheating of a cell or accidents, where the so-called thermal runaway can occur. Temperatures can reach up to 1000 K, well above the boiling temperature of these carbonates. For these battery safety tests and the associated safety simulations, heat capacity data of the cell and its components, such as the two carbonates, are required [3]. With this data the generated heat during the Heat-Wait-Seek test in Accelerating Rate Calorimetry or in simulations the temperature distribution in case of a thermal runaway of a cell in a pack can be determined [4,5]. Even after the regular life of those cells, there is a need for heat capacity data at higher temperatures. Due to the recycling process, which involves the removal of the carbonates through evaporation before the active material can be sorted and recycled [6].

The literature data for EC and EMC are mainly limited to the above mentioned temperature range. For EC the literature heat capacities are mainly limited to 337 K, as there are only a few datapoints above 337 K available. Vasil'ev and Korkhov [7] determined the heat capacity of EC from 298 to 337 K using an adiabatic copper calorimeter container. Ding [8] measured the heat capacities for EC in the range from 288 to 321 K. Chernyak and Clements [9] reported the heat capacity for EC from 383.15 to 398.15 K by Differential Scanning Calorimetry (DSC). Peppel [10] reported the heat capacity for EC at 323 K by a self-built reactor vessel. Vogdanis [11] measured the heat capacities for EC in the range from 180 to 450 K by DSC. Pokorny [12] reported the heat capacities for EC in the range of 262 to 323 also by DSC. For EMC the literature data is limited to 320 K. Ding [8] also measured the heat capacity for EMC 179 to 320 K by modulated DSC using both heating and cooling mode. The literature data is listed in Table 2 for EC and Table 5 for EMC.

Therefore, in this paper the heat capacities of EC and EMC are determined at elevated temperatures using differential scanning calorimetry (DSC). The effect of the supercooled liquid of EC measured in the cooling mode of the DSC on the heat capacity is discussed. It turned out that a simplified Maier–Kelley-fit for the heat capacities of EC and EMC in liquid phase has a good agreement with the experimental data and

* Corresponding author.
E-mail address: philipp.finster@kit.edu (P. Finster).

https://doi.org/10.1016/j.ctta.2025.100170
Received 30 October 2024; Received in revised form 28 January 2025; Accepted 3 February 2025
Available online 17 February 2025

Table 1
Characteristic of sample and reference materials.

Chemical	Composition	Source	Purity
Ethylene carbonate	$C_3H_4O_3$	Sigma-Aldrich	>99%[a]
Ethyl methyl carbonate	$C_4H_8O_3$	Sigma-Aldrich	>99%[a]
Sapphire (reference material)	α-Al_2O_3	Netzsch GmbH	>99.95%[b]

[a] Analysis certificate by Sigma-Aldrich. Certificates are attached in the supplementary.
[b] National Bureau of Standards (NBS), SRM 720.

is therefore provided. Additionally, the melting points, boiling points and the melting enthalpies of EMC and EC were measured.

2. Experimental

2.1. Materials

The measured samples of EC and EMC were purchased from Sigma-Aldrich (St. Louis, MO, USA) and had a purity greater than 99%. The materials are listed in Table 1. The chemicals were stored in an argon filled glovebox to prevent decomposition and possible reactions between the chemicals and oxygen or humidity [10,13]. As reference material sapphire (NIST-SRM α-aluminum oxide) was used [14,15].

2.2. Differential scanning calorimetry (DSC)

The measurements of the heat capacities of EC and EMC were performed with a differential scanning calorimeter. A DSC 204 F1 Phoenix (Netzsch GmbH, Selb, Germany) equipped with a τ-Sensor (constantan disk sensor with E-type thermocouple) was used. It works according to the heat flux principle, where the heat flow rate between sample and reference is a function of temperature. All measurements were carried out under argon 5.0 gas flow of 50 ml/min. To minimize the impact of handling the crucibles, all measurements were performed using the automatic sample changer. The reference crucible remained in its original position throughout the series of experiments, in order to prevent any potential impact of handling. A liquid nitrogen cooling system was used to cool the samples below room temperature. All measurements have been performed with Aluminum concavus crucibles with a diameter of 5 mm and a volume of 40 µl. Aluminum lids were used.

2.2.1. Continuous method

The continuous method is applied for determining the heat capacity. The program was as follows:

1. Heating ramp with 10 K/min rate to required temperature,
2. Holding temperature for 5 min,
3. Cooling ramp with 10 K/min rate to required temperature,
4. Holding temperature for 20 min.

This program is repeated at least three times for every substance.

The temperature range for the measurement of EC was 263 to 500 K for the heating ramp and 493 to 273 K for the cooling ramp. The cooling ramp was used to determine the effect of the supercooled liquid on the heat capacity of EC, as described in the results. For EMC the heat capacity was measured in the heating ramp from 211 to 360 K. As recommended by Hoehne et al. [14] only the second and third heating and cooling ramp were used for calculating the heat capacity. The heat capacity measurement was carried out according to the "three step procedure":

1. Determination of zero line, with empty sample and reference crucible,
2. Measurement of reference substance with known heat capacity in sample crucible and reference crucible empty,
3. Replacing the reference substance by the sample substance and measurement.

The heat capacity was determined according to Eq. (1) with the heat flow rates of the sample (Φ_S), the reference material (Φ_{Ref}), the empty sample and the reference crucibles (Φ_0), the masses of reference (m_{Ref}) and sample (m_S), the heat capacity of the reference material at the specific temperature ($C_{p,Ref}$), the mass of the reference ($m_{cr,Ref}$) and sample crucible ($m_{cr,S}$) and the heat capacity of the crucible material ($C_{p,cr}$):

$$C_{p,Sample} = \frac{\Phi_S - \Phi_0}{\Phi_{Ref} - \Phi_0} \cdot \frac{m_{Ref}}{m_S} \cdot C_{p,Ref} + \frac{m_{cr,Ref} - m_{cr,S}}{m_S} \cdot C_{p,cr} \quad (1)$$

[14]

The crucibles and lids were weighed before the experiment and sorted according to their mass, so that every crucible pair had a mass of about 52 mg. It was important to make sure that every sample and reference crucible had a comparable mass to reduce this possible source of error [14].

The sapphire disc for the reference measurement had a diameter of 4 mm and a mass of 26.25 mg. For calculating the heat capacity, values for sapphire from della Gatta et al. [15] were used. The analysis was done using the Proteus Software in Version 8.0 (Netzsch, Selb, Germany). All samples were prepared in an argon filled glovebox (content of oxygen and water levels lower than 0.1 ppm). The liquid samples were transferred into the crucibles by using a pipette. The lid was attached by using a press. The samples were weighed to ensure a comparable weight of 30 mg for all samples. The crucibles containing the samples were stored in the glovebox. After DSC, the sealed crucibles with samples were weighed again to make sure that no mass change due to evaporation or chemical reaction occured. The procedure was repeated three times both for EC and EMC. For the heat capacity evaluation a level of confidence of 0.95 is used as recommended by Hoehne et al. [14].

$$\frac{p_1}{p_2} = \frac{T_1}{T_2} \quad (2)$$

As the measurement is carried out only 25 K under the boiling point of both carbonates the pressure rises significantly above standard pressure of 100 kPa. Therefore the estimated pressure inside the crucibles is calculated. We assume that the volume of the gas is mostly constant inside the crucible. This allows using the second law of Gay-Lussac (Eq. (2)), which is extended with the vapor pressure of the carbonate at the specific temperature shown in Eq. (3). A pressure of 100 kPa is set for the calculations to 300 K as this is the temperature and pressure inside the glovebox, when the crucibles were closed. For EC the vapor pressure data calculated by Pokorny et al. [12] and Chernyak and Clements [9] were used. For EMC the vapor pressure measured by Zhang et al. [16] was used.

$$p_{exp} = \frac{T_{exp}}{300\ \mathrm{K}} \cdot 100\ \mathrm{kPa} + p_{vap,carb}(T_{exp}) \quad (3)$$

As the vapor pressure is only true for thermal equilibrium, which is not true for experiments with, for instance heating rates, we assume the uncertainty of the calculated pressure to be 0.1 p_{exp}.

2.3. Temperature and enthalpy calibration

The temperature and enthalpy calibration were performed using high purity standard calibration substances, namely Adamantane

($C_{10}H_{16}$), Indium, Tin, Bismuth and Zinc. Adamantane is not recommended by IUPAC, but extensively used and described in the literature for instance by Shimkin [17] and Hoehne et al. [14]. The mass of the calibration substances were chosen according to the expected enthalpy of the melting of the two carbonates as described by Hoehne et al. [14]. The corresponding melting points for the metals and transition point for Adamantane and their enthalpies were used for the calibration. The literature values are summarized in Table A.8 in Appendix. For the determination of the transition temperatures, the extrapolated onset was used, due to its relatively independence of the sample and test parameters according to Hoehne et al. [14]. Because of the five calibration substances a polynomial fit for the temperature and enthalpy calibration was used. The polynomial fit is provided in Eqs. (A.1) and (A.2) in Appendix. The calibration method was described by Shimkin [17] and Drebushchak [18]. For the calculation of the fit, Indium was given a higher weight in the calculation of 10, instead of 1 for the other substances, due to its precisely and accurately known melting point and enthalpy, following the recommendation by Netzsch.

2.3.1. *Determination of melting points, melting enthalpies and boiling points*

Additionally, the melting and boiling points as well as the melting enthalpies of EC and EMC were determined. The similar preparation procedure as described above was used. For determining the boiling points, the lid is punctured directly before the experiment by the automatic sample changer. The punctured lid is used to approximate a quasi constant pressure inside the crucible, according to Seyler [19]. The holes in the lid had a diameter of 0.3 mm, measured by optical microscopy. For the determination of the phase transition temperatures, the sample is cooled well below its melting point with a cooling rate of 20 K/min, followed by an isothermal section of 15 min, to ensure the solidification of the sample. Then the sample was heated up with a heating rate of 10 K/min above its boiling point [15]. The use of the extrapolated onset is due to the calibration technique mentioned above, which also uses the extrapolated onset. The enthalpy of fusion was calculated by integrating the absorption peak area of the measured curve with the baseline subtracted. For both temperature and enthalpy determination a linear baseline was used. The uncertainty of the temperature measurement was estimated to be 0.8 K in the measurement of transition temperatures and 5% for the melting enthalpies according to Hoehne et al. [14]. For EC and EMC three samples each were measured.

3. Results and discussion

The heat capacity of EC measured in the temperature range between 263 to 500 K within the heating ramp is given in Table 3. The uncertainties correspond, as discussed before, to the confidence interval of 0.95 and are between 5.4 (263 K) and 8.9 J K^{-1} mol^{-1} (500 K). The heat capacity values given in Table 3 are the average values of the second and third heating stage for the three samples. In Table 3 the heat capacity is only shown in 5 K intervals for readability. The measured heat capacity in 1 K steps for the heating and cooling mode is attached in Tables A.9 and A.11 in Appendix. An overview of the literature data is given in Table 2.

As the heat capacity curve of EC is mostly linear in the liquid phase and for the supercooled liquid, a linear fit is provided using only the two factors A and B of the Maier–Kelley-equation in the temperature range 273 to 500 K:

$$C_{p,m}\,/\mathrm{J\ K^{-1}\ mol^{-1}} = A + B \cdot T + C \cdot T^{-2} \quad (4)$$

With the following coefficients:

$A = 77.41 \pm 0.38$

$B = 0.196 \pm 1{\cdot}10^{-3}$

The coefficients were determined by weighted least squares method (Origin Pro Software Ver 2022) using the experimental heat capacity data of this work in heating and cooling mode, as well as the literature data, which is inside the confidence interval of our measurements, as described in the following paragraph. The weighting factor was $\frac{1}{\delta^2}$, where δ is the reported uncertainty. When no uncertainty was reported an uncertainty of 0.05 $C_{p,m}$ was used as weight for the calculation of the fit. The fit is plotted together with experimental and literature data in Fig. 2 and for better readability as deviation plot in Fig. 3.

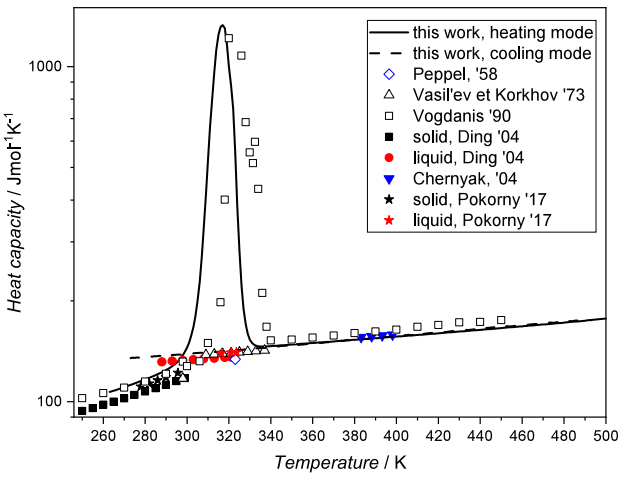

Fig. 1. Heat capacity data and melting peak for EC ($C_{p,m}$/(J K^{-1} mol^{-1}) as a function of temperature using a logarithmic scale. Values from literature by Peppel [10], Vasil'ev and Korkhov [7], Ding [8], Chernyak et al. [9], Vogdanis [11] and Pokorny [12] are shown for comparison.

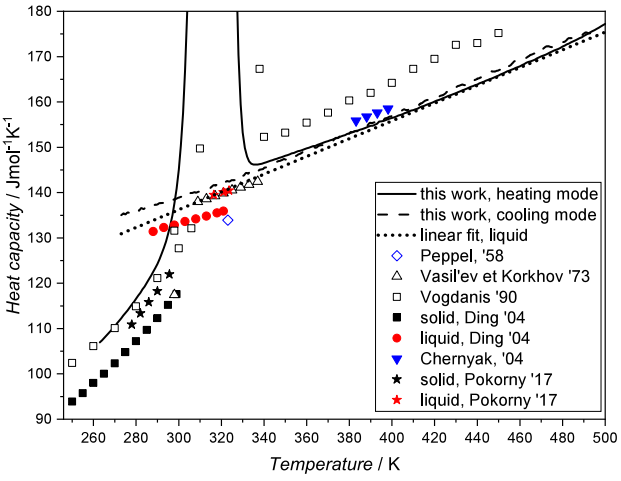

Fig. 2. Heat capacity data and melting peak for EC ($C_{p,m}$/(J K^{-1} mol^{-1}) as a function of temperature using a linear scale. Values from literature by Peppel [10], Vasil'ev and Korkhov [7], Ding [8], Chernyak et al. [9], Vogdanis [11], Pokorny [12] and the linear fit for comparison.

The experimental heat capacity data of this work are shown together with literature data for comparison in Fig. 1. Our results are in the same order of magnitude as the literature data of Vasilev and Korkhov [7], Chernyak et al. [9] and Pokorny [12]. The data of Vogdanis [11] above 400 K and the data of Peppel [10] are outside of the confidence interval of our DSC measurement in the liquid phase. The deviation is 5.2% at 410 K and 6% at 440 K for Vogdanis [11] and −6.2% at 323 K for Peppel [10]. The deviation of Vogdanis [11] to the other literature data cited in this work is in the same range for a temperature of 340 K. The highest deviation between the literature data, except the data of Vogdanis [11] and Peppel [10], in the liquid phase is at 321 K with −3.2% to the data of Ding [8]. For the data of Chernyak [9] and Vogdanis [11] the deviation at 390 K is 2.2% and 5.3% respectively. Therefore we assume that our new experimental data for the liquid state of EC gives new data above 450 K and is in good agreement

Table 2
Overview of the literature solid and liquid heat capacity for Ethylene Carbonate.

Reference	N[a]	*Temperature* K	$u_r(C_{p,m})$[b] %	mole fraction purity	Method
Ethylene Carbonate, Solid Phase					
Vasil'ev & Korkhov [7]	1	298.48	n/a[c]	0.9983	adiabatic
Ding [8]	S[d]	250.00–299.00	5.0	0.9998	DSC
Vogdanis [11]	22	180.00–306.00	5.0	n/a	DSC
Pokorny [12]	18	262.19–295.68	1.0	1.000	Tian-Calvet
this work	26	263.15–289.15	5.0	0.999	DSC
Ethylene Carbonate, Liquid Phase					
Vasil'ev & Korkhov [7]	16	309.48–337.98	n/a[c]	0.9983	adiabatic
Ding [8]	S[d]	310.00–321.00	5.0	0.9998	DSC
Chernyak & Clements [9]	4	383.15–398.15	2.5	0.999	DSC
Peppel [10]	1	323.15	n/a[c]	0.99	self-built reactor vessel
Vogdanis [11]	13	340.00–450.00	5.0	n/a	DSC
Pokorny [12]	9	316.43–323.60	1.0	1.000	Tian-Calvet
this work	162	338.15–500.15	5.0	0.999	DSC

[a] N stands for number of data points.
[b] $u_r(C_{p,m})$ stands for relative uncertainty as stated by the authors.
[c] n/a stands for not available.
[d] S stands for smoothed data.

Table 3
Experimental heat capacities of EC and calculated pressure inside crucible in the temperature range between 263 and 500 K.[a]

Ethylene Carbonate, Solid Phase					
T/K	$C_{p,m}$ J K^{-1} mol^{-1}	p kPa	T/K	$C_{p,m}$ J K^{-1} mol^{-1}	p kPa
263.15	107.0	87.6	278.15	115.3	92.6
268.15	109.4	89.6	283.15	118.6	93.4
273.15	112.2	91.0	288.15	122.5	96.0
Ethylene Carbonate, Liquid Phase					
T/K	$C_{p,m}$ J K^{-1} mol^{-1}	p kPa	T/K	$C_{p,m}$ J K^{-1} mol^{-1}	p kPa
338.15	146.3	112.7	423.15	160.6	146.9
343.15	147.0	114.4	428.15	161.6	149.8
348.15	147.8	116.1	433.15	162.6	152.8
353.15	148.6	117.9	438.15	163.5	156.0
358.15	149.4	119.6	443.15	164.5	159.5
363.15	150.2	121.3	448.15	165.4	163.2
368.15	151.0	123.1	453.15	166.5	167.2
373.15	151.9	124.9	458.15	167.5	171.5
378.15	152.7	126.7	463.15	168.6	176.2
383.15	153.6	128.6	468.15	169.6	181.4
388.15	154.3	130.6	473.15	170.6	187.0
393.15	155.2	132.6	478.15	171.7	193.3
398.15	156.1	134.7	483.15	172.9	200.2
403.15	157.0	136.8	488.15	174.1	207.9
408.15	157.9	139.2	493.15	175.4	216.4
413.15	158.8	141.6	498.15	176.7	255.9
418.15	159.7	144.2			

[a] Standard uncertainty is $u(T) = 0.8$ K, $u(p) = 0.1$ p and the combined expanded uncertainty of the heat capacity is $U_c(C_{p,m}) = 0.05$ $C_{p,m}$ (0.95 level of confidence).

Table 4
Calculated slops of the linear fit, the heat capacity data of this work below the melting point (cooling mode), the data of Ding [8] (liquid), Vasil'ev et Korkhov [7], Chernyak et al [9], Vogdanis [11] and Pokorny [12] for EC.

Data	Slope	Deviation
Linear fit for EC this work (cool mode & T < T_{melt})	0.196 0.145	$\pm 1 \cdot 10^{-3}$ $\pm 1.2 \cdot 10^{-3}$
Ding, liquid [8]	0.133	$\pm 2.6 \cdot 10^{-3}$
Vasil'ev et Korkhov [7]	0.159	$\pm 1.18 \cdot 10^{-5}$
Chernyak [9]	0.176	$\pm 2.2 \cdot 10^{-15}$
Vogdanis [11]	0.221	$\pm 5.5 \cdot 10^{-3}$
Pokorny [12]	0.133	$\pm 3.3 \cdot 10^{-3}$

with the literature, except the data of Vogdanis [11] and Peppel [10]. Therefore the literature data except of Vogdanis [11] and Peppel [10] were used to determine the provided linear fit. The correction for vaporization of the carbonate at higher temperatures inside the crucible was investigated for EC using the approach of Paramo et al. [20], which is described in the supplementary. As the calculated error is highest at 500 K with −0.15%, which is over twenty times lower than the expanded uncertainty, the experimental values were not corrected. The overlap between the heat capacity for solid and liquid phase measured in heating and cooling mode in this work and by Ding [8] is due to the fact that measuring in the cooling mode leads to supercooling effects in the liquid EC. Therefore the data below the melting point is referred as metastable liquid. In Fig. 2 there is a change in the slope of the heat capacity data for the cooling mode below the melting point visible. The slope of the heat capacity below the melting point shows the same

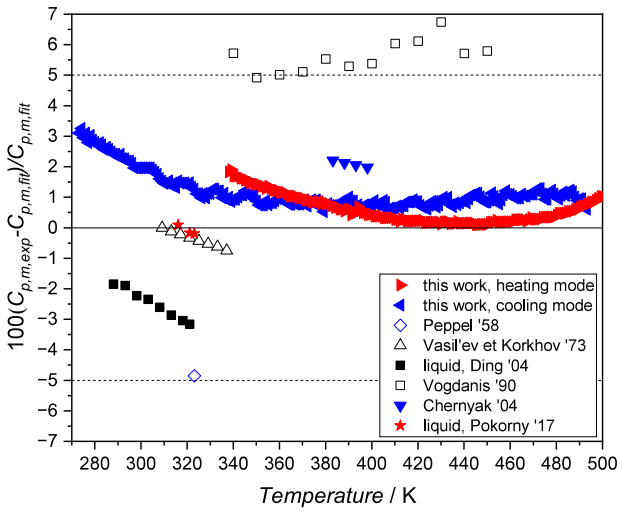

Fig. 3. Relative deviation $100(C_{p,m,exp}\text{-}C_{p,m,fit})/C_{p,m,fit}$ of individual experimental heat capacities $C_{p,m,exp}$ from values of the fit calculated with Eq. (4) for EC.

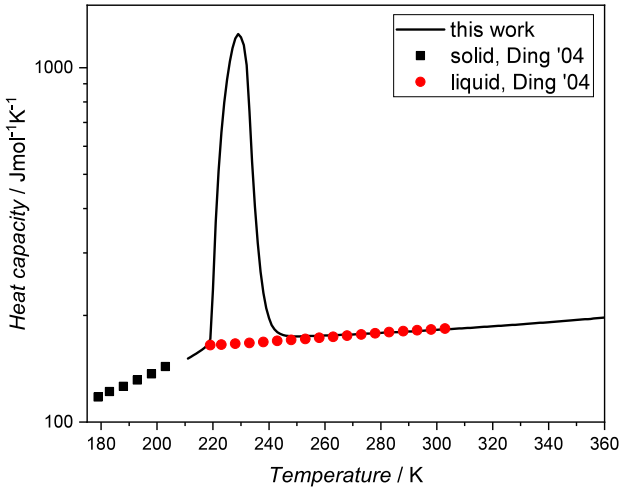

Fig. 4. Heat capacity data for EMC ($C_{p,m}$/(J K^{-1} mol^{-1}) as a function of temperature using a logarithmic scale. Values from literature by Ding [8] for comparison.

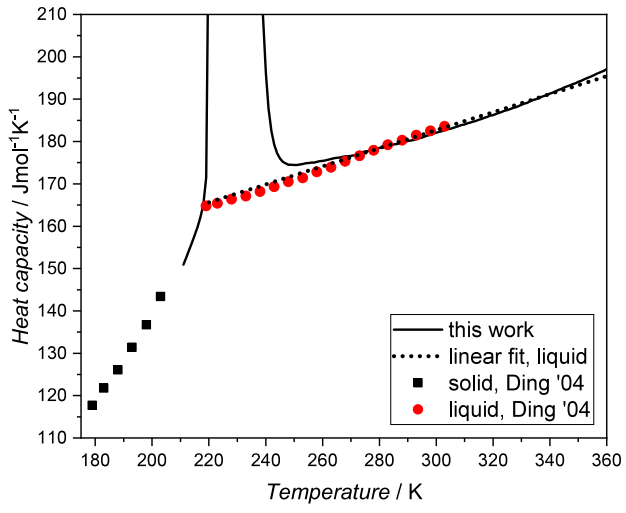

Fig. 5. Heat capacity data and melting peak for EMC ($C_{p,m}$/(J K^{-1} mol^{-1}) as a function of temperature using a linear scale. Values from literature by Ding [8] and the linear fit for comparison.

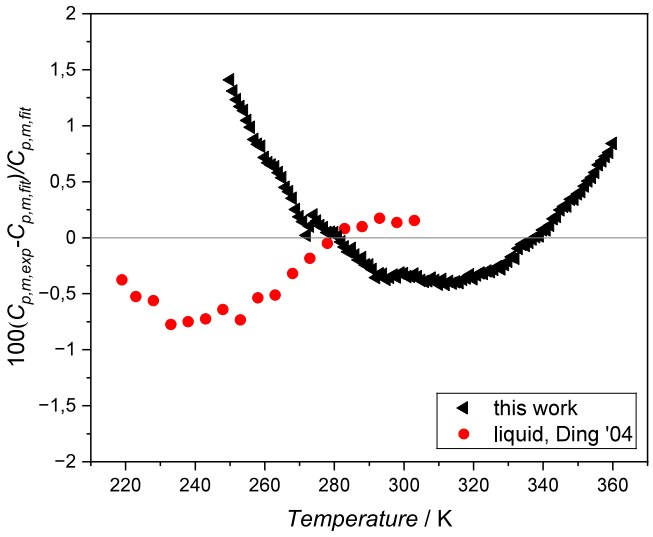

Fig. 6. Relative deviation $100(C_{p,m,exp}\text{-}C_{p,m,fit})/C_{p,m,fit}$ of individual experimental heat capacities $C_{p,m,exp}$ from values of the fit calculated with Eq. (4) for EMC.

range as the slope of the data of Ding [8] measured also in the cooling mode and Pokorny [12]. The slope of the data of Pokorny might be in this range because they only reported a few data points in a small temperature range. Since the deviation between the linear fit and our experimental data is highest at 273 K with 1.6% only of one third of the expanded uncertainty of 0.5 $C_{p,m}$ we assume that the linear fit is also suitable for the supercooled liquid. The slope of the heat capacity higher than the melting point correlates well with the slope of the data of Vasil'ev et Korhkov [7], Chernyak [9] and Vogdanis [11]. The calculated slopes using the least square method of the provided fit, our data for the heat capacity below the melting point, the data of Ding [8], Vasil'ev et Korkhov [7], Chernyak [9], Vogdanis [11] and Pokorny [12] are listed in Table 4 for comparison.

The heat capacity of EMC measured in the temperature range between 211 to 360 K is given in Table 6. The uncertainties correspond to a confidence interval of 0.95 and are between 7.5 J K^{-1} mol^{-1} (211 K) and 10.0 J K^{-1} mol^{-1} (360 K). As for EC the heat capacity values given in Table 6 are the average values of the second and third heating step for the three samples. In Table 6 the heat capacity is only shown in 5 K intervals for readability. The measured heat capacity in 1 K steps is given in Table A.10 in Appendix.

For EMC a linear behavior of the heat capacity in the liquid phase was found. Similarly, a linear fit using the two coefficients A and B of Eq. (2) can be made based on the experimental data of this work and the data of Ding [21] with the coefficients in the temperature range of 220 to 360 K:

A = 118.77 ± 0.65

B = 0.213 ± 2.2·10^{-3}

The heat capacity data are shown in the same way as for EC in Fig. 4 together with the literature data. The data are plotted together with the linear fit in Fig. 5 and for better readability as deviation plot in Fig. 6.

The results show a good agreement with the literature data and give new experimental data for elevated temperatures below the boiling point. The literature data from Ding [8] for the liquid phase show data points in the range of the melting peak, this is due to the measurement in the cooling mode. This was chosen by Ding because, as discussed in the introduction, the temperature range of regular use of EMC is below 333 K. As the data of Ding [8] fits well with our data the calculated fit has been extrapolated into the temperature range of the data of Ding and shows very good agreement. As well as for EC the correction for

Table 5
Overview of the literature solid and liquid heat capacity for Ethyl Methyl Carbonate.

Reference	N[a]	$Temperature$ K	$u_r(C_{p,m})$[b] %	mole fraction purity	Method
Ethyl Methyl Carbonate, Solid Phase					
Ding [8]	S[c]	179.00–203.00	5.0	0.9998	DSC
this work	6	211.15–216.15	5.0	0.996	DSC
Ethylene Carbonate, Liquid Phase					
Ding [8]	S[c]	310.00–321.00	5.0	0.9998	DSC
This work	110	250.15–360.15	5.0	0.996	DSC

[a] N stands for number of data points. [b] $u_r(C_{p,m})$ stands for relative uncertainty as stated by the authors. [c] S stands for smoothed data.

Table 6
Experimental heat capacities of EMC measured in the temperature range between 211 K and 360 K.[a]

Ethyl Methyl Carbonate, Solid Phase					
T/K	$C_{p,m}$ J K^{-1} mol^{-1}	p kPa	T/K	$C_{p,m}$ J K^{-1} mol^{-1}	p kPa
211.15	150.9	70.3	216.15	159.8	72.0
Ethyl Methyl Carbonate, Liquid Phase					
T/K	$C_{p,m}$ J K^{-1} mol^{-1}	p kPa	T/K	$C_{p,m}$ J K^{-1} mol^{-1}	p kPa
250.15	174.4	83.5	310.15	184.0	109.7
255.15	174.9	85.2	315.15	185.1	113.1
260.15	175.4	87.0	320.15	186.2	116.9
265.15	176.2	88.8	325.15	187.4	121.2
270.15	176.6	90.6	330.15	188.7	126.0
275.15	177.6	92.5	335.15	190.0	132.6
280.15	178.5	94.5	340.15	191.3	137.5
285.15	179.3	96.6	345.15	192.7	144.4
290.15	180.1	98.8	350.15	194.1	152.3
295.15	180.9	101.2	355.15	195.5	161.1
300.15	182.1	103.8	360.15	197.1	171.1
305.15	183.0	106.6			

[a] Standard uncertainty is $u(T) = 0.8$ K, $u(p) = 0.1$ p and the combined expanded uncertainty of the heat capacity is $U_c(C_{p,m}) = 0.05$ $C_{p,m}$ (0.95 level of confidence).

Table 7
Measured and literature data for phase transition of ethylene carbonate and ethyl methyl carbonate.[a].

Chemical	T_{melt}/K Experiment	T_{melt}/K Literature
EC	309.2 ± 0.8	310 [13]
EMC	219.7 ± 0.8	219 [8]
Chemical	$\Delta_{fus}H$/kJ mol^{-1} Experiment	$\Delta_{fus}H$/kJ mol^{-1} Literature
EC	13.3 ± 0.7	13.02 [8], 13.30 [7]
EMC	11.5 ± 0.6	11.24 [8]
Chemical	T_{boil}/K Experiment	T_{boil}/K Literature
EC	523.2 ± 0.8	511 [13], 523 [21]
EMC	384.6 ± 0.8	383 [21]

[a] Standard uncertainty is $u(T) = 0.8$ K, and the combined expanded uncertainty of the enthalpy of fusion is $U_c(\Delta_{fus}H) = 0.05$ $\Delta_{fus}H$ (0.95 level of confidence).

vaporization of the carbonate at higher temperatures inside the crucible was investigated using the approach of Paramo et al. [20], which is described in the supplementary. As the calculated error is highest at 360 K with −0.5%, which is over ten times lower than the expanded uncertainty, the experimental values were not corrected.

In Table 7 the measured transition points and melting enthalpies are listed together with the literature data for comparison.

The measured melting temperatures and enthalpies agree very well with the literature data. The boiling point of EMC also shows a good agreement with the literature data. For the boiling point of EC, temperatures between 511 and 523 K have been reported in literature by Wang [13] and Ding [21]. Also there is discussion, for instance by Wang [13], that the decomposition of EC starts right above the boiling point. Therefore the empty crucible was checked by visual

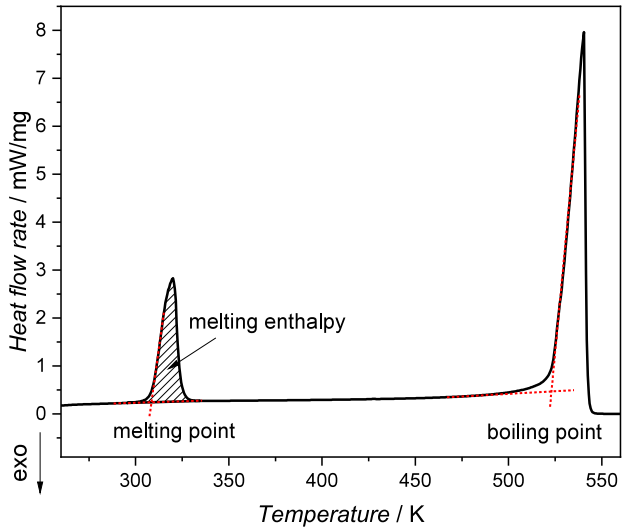

Fig. 7. Determination of the melting, boiling point and melting enthalpy for EC.

inspection after the experiment and no decomposition products where found. In the DSC curve in Fig. 7 there was also no other peak than the expected one visible. We assume that the measured boiling point is with respect to the accuracy of the experiment and the determination by the extrapolated onset correct. Moreover with the vapor pressure data of Chernyak and Clements [9] with the highest vapor pressure of 73.45 kPa at 505 K, we extrapolated the data to higher temperatures and found that the calculated vapor pressure at 511 K is only 86.2 kPa. Therefore we assume that the measured boiling point of EC is correct. The calculation is described in the supplementary. The sharp boiling peak of the EC and EMC in the measurements show that the used diameter of the hole in the lid of the crucible and the mass of the sample are sufficient for the measurement [19].

4. Conclusion

This study presents heat capacity data at elevated temperatures for EC and EMC both measured using the continuous method on a Netzsch DSC 204 F1 Phoenix for the liquid phase. For EC the measured temperature range was between 263 and 500 K in the heating mode and 493 to 273 K in the cooling. For EMC the measurement was performed between 211 and 360 K. The results show a good agreement with most of the literature data and represent new experimental data for elevated temperatures above 337 K. A simplified Maier–Kelley-fit for EC and EMC liquid phase respectively, was provided in the temperature range from 273 to 500 K for EC and from 220 to 360 K for EMC. Moreover the supercooling of EC and the effect on the slope of the heat capacity data were discussed and assumed that the provided fit is, with respect to the deviation of the experiment, also applicable for the metastable liquid of EC. The melting temperatures and enthalpies were measured and show a good agreement with the literature, as well as the boiling point for EMC and EC.

The enhanced temperature range of the heat capacity of EC and EMC gives key input data for safety simulations, calculations and battery management systems to calculate the behavior of cells at elevated temperatures above 337 K.

CRediT authorship contribution statement

Philipp Finster: Writing – original draft, Visualization, Methodology, Investigation, Conceptualization. **Judith Jung:** Investigation. **Magnus Rohde:** Validation, Supervision, Resources. **Hans Jürgen Seifert:** Writing – review & editing, Validation, Supervision, Resources, Funding acquisition. **Carlos Ziebert:** Writing – review & editing, Supervision, Funding acquisition.

Declaration of competing interest

The authors declare that they have no known competing financial interests or personal relationships that could have appeared to influence the work reported in this paper.

Acknowledgments

This project was partly funded by the German Federal Ministry of Education and Research within the Competence Cluster Battery Utilization Concepts (BattNutzung) under the grant number 03XP0311A.

This research was partly funded by the Helmholtz Association, Germany, grant number FE.5341.0118.0012, in the programme Materials and Technologies for the Energy Transition (MTET), and we want to express our gratitude for the funding. We thank the members of the group Batteries – Calorimetry and Safety of the IAM-AWP for the fruitful discussions.

This work contributes to the research performed at CELEST (Center of Electrochemical Energy Storage Ulm-Karlsruhe).

Appendix. Supplementary data

A.1. Calibration

The polynomial fit for the temperature calibration of the DSC:

$$T_{corr} = 10^{-3} \cdot B_0 + 10^{-5} \cdot B_1 \cdot T_{exp} + 10^{-8} \cdot B_2 \cdot T_{exp}^2 \quad \text{(A.1)}$$

with the coefficients $B_0 = -563.0$, $B_1 = -336.3$ and $B_3 = -3.8$.

The polynomial fit for the enthalpy calibration of the DSC:

$$y = (P_2 + P_3 \cdot z + P_4 \cdot z^2 + P_5 \cdot z^3) exp^{-z^2} \text{ and } z = (T_{exp} - P_0)/P_1 \quad \text{(A.2)}$$

with the coefficients $P_0 = -64.5$, $P_1 = 1013.25934$, $P_2 = 3.17643$, $P_3 = 1.06348$, $P_4 = -1.66090$ and $P_5 = -1.18169$.

A.2. Influence of vaporization on the experiment

The influence of vaporization of the two carbonates inside the crucibles at elevated temperatures can be determined using Eq. (A.3), which was introduced and described by Paramo et al. [20].

$$C_t = n^l c_{sat}^l + n^g c_{sat}^g + \Delta H (\frac{\delta n^g}{\delta T})_{sat} \quad \text{(A.3)}$$

As the measured heat capacity consists of the heat capacity of the liquid and gaseous phase and the vaporization enthalpy of the carbonate which is evaporated due to the rising vapor pressure of the carbonate with temperature. We assumed a volume of 30 µl of carbonate in the crucible as the density of both carbonates are between 1.0 and 1.3 at ambient temperature. As there was a crucible used with 40 µl volume the rest 10 µl must be the volume of the gas phase. Using the known temperature (T) in the experiment, the pressure (p), which is in this case the vapor pressure of the carbonate, the volume of the gas phase (V) and the gas constant R_m, we can calculate the amount in mole of carbonate in the gas phase (n) and with the change of amount in the gas phase the influence of $\Delta H(\frac{\delta n^g}{\delta T})_{sat}$ using the ideal gas law adjusted in Eq. (A.4):

$$n = \frac{p \cdot V}{R_m \cdot T} \quad \text{(A.4)}$$

Table A.8
Reference materials applied for the temperature and enthalpy calibration of the DSC 204 and their transition points and enthalpies.

Substance	Transition point T/K	Transition enthalpy kJ/mol
Adamantane $C_{10}H_{16}$	208.7	2.997
Indium	429.8	3.284
Tin	505.1	7.182
Bismuth	544.6	11.10
Zinc	692.7	7.029

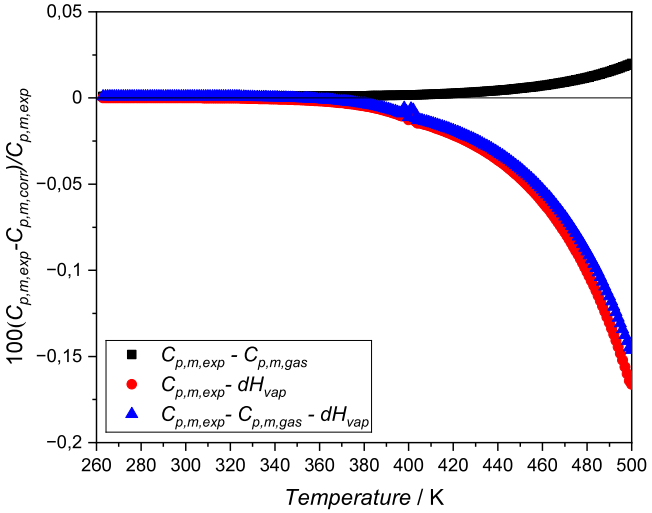

Fig. A.8. Relative deviation $100(C_{p,m,exp}\text{-}C_{p,m,corr})/C_{p,m,exp}$ of individual values of correction terms for gas phase and enthalpy of vaporization calculated with Eq. (A.3) from values of the experimental heat capacities $C_{p,m,exp}$ for EC.

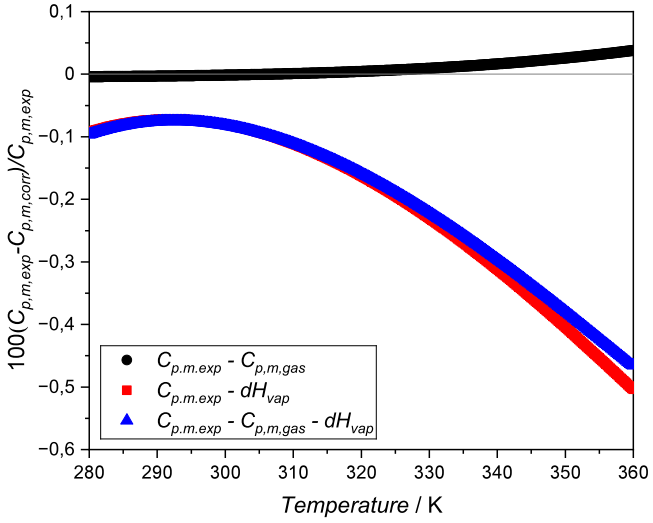

Fig. A.9. Relative deviation $100(C_{p,m,exp}\text{-}C_{p,m,corr})/C_{p,m,exp}$ of individual values of correction terms for gas phase and enthalpy of vaporization calculated with Eq. (A.3) from values of the experimental heat capacities $C_{p,m,exp}$ for EMC.

The vapor pressure data was the same used for the determination of the pressure inside the crucibles for both carbonates. The heat capacity for the gas phase was calculated using the Joback-method described for both carbonates by Baakes et al. [22]. The used enthalpies of vaporization were 58.7 kJ/mol for EC and 36.1 kJ/mol for EMC calculated also by Braakes et al. [22].

It turned out that for both carbonates the influence is lower than −0.15% for EC (Fig. A.8) and −0.5% for EMC (Fig. A.9) which is a minimum of 10 times lower than the expanded uncertainty of 0.05 $C_{p,m}$. Therefore no correction for the influence of the gasphase and enthalpy of vaporization was performed.

A.3. Calculation of the boiling point of EC with vapor pressures

The vapor pressure at 508 K was calculated using a fit on the literature data of Chernyak and Clements [9] with the following equation:

$$p_{vap} = B \cdot exp^{(-T/t_1)} + A \quad \text{(A.5)}$$

With the following coefficients:
$A = -6.61 \pm 0.55$
$B = 3.83 \pm 6.4{\cdot}10^{-5}$
$t_1 = -41.27 \pm 0.54$

The coefficients were determined by least squares method (Origin Pro Software Ver 2022). As the boiling point reported from Wang et al. [13] is only 3 K above the measured vapor pressures by Chernyak and Clements [9] we assume that the fit is suitable for this temperature range as showed in Fig. A.10.

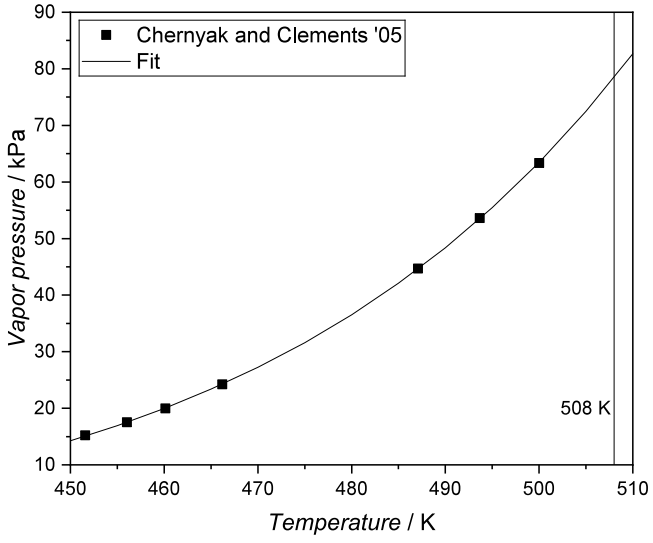

Fig. A.10. Calculated vapor pressure of EC at 508 K with fit of Eq. (A.5) based on the literature data of Chernyak and Clements [9].

A.4. Heat capacity data in 1 K steps

See Figs. A.11 and A.12.

Table A.9
Experimental heat capacities of EC and calculated pressure inside crucible in the temperature range between 263 and 500 K measured by DSC 204 in the heating mode[a].

Ethylene Carbonate, Solid Phase					
T/K	$C_{p,m}$ J K^{-1} mol^{-1}	p kPa	T/K	$C_{p,m}$ J K^{-1} mol^{-1}	p kPa
263.15	107.0	85.5	277.15	114.6	90.2
264.15	107.4	85.8	278.15	115.3	90.6
265.15	107.9	86.2	279.15	115.9	90.9
266.15	108.4	86.5	280.15	116.6	91.2
267.15	108.9	86.8	281.15	117.3	91.6
268.15	109.4	87.2	282.15	117.9	91.9
269.15	109.9	87.5	283.15	118.6	92.2
270.15	110.4	87.9	284.15	119.3	92.6
271.15	111.1	88.2	285.15	120.1	92.9
272.15	111.7	88.5	286.15	120.9	93.3
273.15	112.2	88.9	287.15	121.6	93.6
274.15	112.9	89.2	288.15	122.5	93.9
275.15	113.4	89.5	289.15	123.3	94.3
276.15	114.0	89.9			
Ethylene Carbonate, Liquid Phase					
T/K	$C_{p,m}$ J K^{-1}mol^{-1}	p kPa	T/K	$C_{p,m}$ J K^{-1}mol^{-1}	p kPa
338.15	146.3	111.2	420.15	160.1	145.3
339.15	146.6	111.6	421.15	160.3	145.8
340.15	146.5	111.9	422.15	160.5	146.4
341.15	146.7	112.3	423.15	160.6	146.9
342.15	146.9	112.6	424.15	160.8	147.5
343.15	147.0	113.0	425.15	161.0	148.0
344.15	147.2	113.4	426.15	161.2	148.6
345.15	147.3	113.7	427.15	161.4	149.2
346.15	147.5	114.1	428.15	161.6	149.8
347.15	147.6	114.4	429.15	161.8	150.4
348.15	147.8	114.8	430.15	161.9	151.0
349.15	147.9	115.2	431.15	162.2	151.6
350.15	148.1	115.5	432.15	162.4	152.2
351.15	148.3	115.9	433.15	162.6	152.8
352.15	148.4	116.3	434.15	162.7	153.4
353.15	148.6	116.6	435.15	162.9	154.1
354.15	148.7	117.0	436.15	163.1	154.7
355.15	149.0	117.4	437.15	163.4	155.3
356.15	149.1	117.7	438.15	163.5	156.0
357.15	149.2	118.1	439.15	163.7	156.7
358.15	149.4	118.5	440.15	163.9	157.4
359.15	149.6	118.8	441.15	164.1	158.0
360.15	149.7	119.2	442.15	164.3	158.7
361.15	149.9	119.6	443.15	164.5	159.5
362.15	150.1	120.0	444.15	164.7	160.2
363.15	150.2	120.3	445.15	164.8	160.9
364.15	150.3	120.7	446.15	165.0	161.6
365.15	150.5	121.1	447.15	165.2	162.4
366.15	150.7	121.5	448.15	165.4	163.2
367.15	150.9	121.9	449.15	165.6	163.9
368.15	151.0	122.2	450.15	165.8	164.7
369.15	151.2	122.6	451.15	166.1	165.5
370.15	151.4	123.0	452.15	166.3	166.3
371.15	151.5	123.4	453.15	166.5	167.2
372.15	151.7	123.8	454.15	166.8	168.0
373.15	151.9	124.2	455.15	166.9	168.8
374.15	152.0	124.6	456.15	167.1	169.7
375.15	152.2	125.0	457.15	167.3	170.6
376.15	152.4	125.4	458.15	167.5	171.5
377.15	152.6	125.8	459.15	167.7	172.4
378.15	152.7	126.2	460.15	167.9	173.3
379.15	153.0	126.6	461.15	168.1	174.3
380.15	153.1	127.0	462.15	168.4	175.2
381.15	153.3	127.4	463.15	168.6	176.2
382.15	153.4	127.8	464.15	168.8	177.2
383.15	153.6	128.2	465.15	169.0	178.2
384.15	153.7	128.6	466.15	169.2	179.2
385.15	153.9	129.0	467.15	169.3	180.3
386.15	154.0	129.4	468.15	169.6	181.4
387.15	154.2	129.8	469.15	169.9	182.5
388.15	154.3	130.2	470.15	170.0	183.6

(*continued on next page*)

Table A.9 (*continued*).

Ethylene Carbonate, Solid Phase					
389.15	154.6	130.7	471.15	170.2	184.7
390.15	154.8	131.1	472.15	170.4	185.9
391.15	154.7	131.5	473.15	170.6	187.0
392.15	155.0	131.9	474.15	170.9	188.2
393.15	155.2	132.4	475.15	171.1	189.5
394.15	155.7	132.8	476.15	171.3	190.7
395.15	155.7	133.2	477.15	171.5	192.0
396.15	155.8	133.7	478.15	171.7	193.3
397.15	156.0	134.1	479.15	171.9	194.6
398.15	156.1	134.6	480.15	172.2	196.0
399.15	156.3	135.0	481.15	172.5	197.3
400.15	156.5	135.5	482.15	172.7	198.8
401.15	156.6	135.9	483.15	172.9	200.2
402.15	156.8	136.4	484.15	173.1	201.7
403.15	157.0	136.8	485.15	173.4	203.2
404.15	157.2	137.3	486.15	173.6	204.7
405.15	157.3	137.8	487.15	173.8	206.3
406.15	157.5	138.2	488.15	174.1	207.9
407.15	157.7	138.7	489.15	174.3	209.5
408.15	157.9	139.2	490.15	174.6	211.2
409.15	158.1	139.7	491.15	174.9	212.9
410.15	158.2	140.2	492.15	175.1	214.6
411.15	158.4	140.6	493.15	175.4	216.4
412.15	158.5	141.1	494.15	175.6	218.2
413.15	158.8	141.6	495.15	175.9	220.1
414.15	159.0	142.1	496.15	176.1	222.0
415.15	159.1	142.7	497.15	176.4	224.0
416.15	159.3	143.2	498.15	176.7	225.9
417.15	159.5	143.7	499.15	177.0	228.0
418.15	159.7	144.2	500.15	177.2	230.1
419.15	159.9	144.7			

[a] Standard uncertainty is $u(T)$ = 0.8 K, $u(p)$ = 0.1 p and the combined expanded uncertainty of the heat capacity is $U_c(C_{p,m})$ = 0.05 $C_{p,m}$ (0.95 level of confidence).

Table A.10
Experimental heat capacities of EMC (211 to 360 K) measured using DSC 204 in the heating mode[a].

Ethyl Methyl Carbonate, Solid Phase					
T/K	$C_{p,m}$ J K^{-1} mol^{-1}	p kPa	T/K	$C_{p,m}$ J K^{-1} mol^{-1}	p kPa
211.15	150.9	70.3	214.15	156.0	71.3
212.15	152.6	70.7	215.15	157.9	71.7
213.15	154.2	71.0	216.15	159.8	72.0
Ethyl Methyl Carbonate, Liquid Phase					
T/K	$C_{p,m}$ J K^{-1} mol^{-1}	p kPa	T/K	$C_{p,m}$ J K^{-1} mol^{-1}	p kPa
250.15	174.4	83.5	306.15	183.2	107.2
251.15	174.5	83.8	307.15	183.5	107.8
252.15	174.6	84.2	308.15	183.7	108.4
253.15	174.7	84.5	309.15	183.9	109.0
254.15	174.8	84.8	310.15	184.0	109.7
255.15	174.9	85.2	311.15	184.3	110.3
256.15	175.0	85.5	312.15	184.5	111.0
257.15	175.0	85.9	313.15	184.7	111.7
258.15	175.2	86.3	314.15	184.9	112.4
259.15	175.4	86.6	315.15	185.1	113.1
260.15	175.4	87.0	316.15	185.3	113.8
261.15	175.5	87.3	317.15	185.6	114.6
262.15	175.7	87.7	318.15	185.8	115.3
263.15	175.9	88.0	319.15	186.1	116.1
264.15	176.0	88.4	320.15	186.2	116.9
265.15	176.2	88.8	321.15	186.5	117.7
266.15	176.2	89.1	322.15	186.8	118.6
267.15	176.4	89.5	323.15	187.0	119.4
268.15	176.5	89.9	324.15	187.2	120.3
269.15	176.5	90.2	325.15	187.4	121.2
270.15	176.6	90.6	326.15	187.7	122.1
271.15	176.7	91.0	327.15	187.9	123.0
272.15	176.7	91.4	328.15	188.1	124.0
273.15	177.1	91.7	329.15	188.4	125.0
274.15	177.5	92.1	330.15	188.7	126.0
275.15	177.6	92.5	331.15	188.9	127.0

(*continued on next page*)

Table A.10 (*continued*).

Ethyl Methyl Carbonate, Solid Phase					
276.15	177.7	92.9	332.15	189.1	128.1
277.15	177.9	93.3	333.15	189.5	129.2
278.15	178.1	93.7	334.15	189.8	130.3
279.15	178.3	94.1	335.15	190.0	131.4
280.15	178.5	94.5	336.15	190.3	132.6
281.15	178.6	94.9	337.15	190.5	133.8
282.15	178.8	95.3	338.15	190.8	150.0
283.15	178.9	95.8	339.15	191.0	163.2
284.15	179.0	96.2	340.15	191.3	137.5
285.15	179.3	96.6	341.15	191.5	138.8
286.15	179.4	97.0	342.15	191.8	140.2
287.15	179.5	97.5	343.15	192.2	141.6
288.15	179.8	97.9	344.15	192.4	143.0
289.15	179.9	98.4	345.15	192.7	144.4
290.15	180.1	98.8	346.15	193.0	145.9
291.15	180.2	99.3	347.15	193.2	147.5
292.15	180.3	99.8	348.15	193.6	149.0
293.15	180.6	100.2	349.15	193.8	150.6
294.15	180.8	100.7	350.15	194.1	152.3
295.15	180.9	101.2	351.15	194.3	154.0
296.15	181.2	101.7	352.15	194.6	155.7
297.15	181.4	102.2	353.15	194.9	157.4
298.15	181.6	102.7	354.15	195.2	159.3
299.15	181.9	103.2	355.15	195.5	161.1
300.15	182.1	103.8	356.15	195.9	163.0
301.15	182.2	104.3	357.15	196.1	165.0
302.15	182.5	104.9	358.15	196.4	167.0
303.15	182.7	105.4	359.15	196.7	169.0
304.15	182.9	106.0	360.15	197.1	171.1
305.15	183.0	106.6			

[a] Standard uncertainty is $u(T) = 0.8$ K, $u(p) = 0.1\ p$ and the combined expanded uncertainty of the heat capacity is $U_c(C_{p,m}) = 0.05\ C_{p,m}$ (0.95 level of confidence).

Table A.11
Experimental heat capacities of EC and calculated pressure inside crucible in the temperature range between 273 and 493 K measured by DSC 204 in the cooling mode[a].

Ethylene Carbonate, Liquid Phase and metastable liquid					
T/K	$C_{p,m}$ J K^{-1} mol^{-1}	p kPa	T/K	$C_{p,m}$ J K^{-1} mol^{-1}	p kPa
273.15	135.0	88.9	384.15	153.7	128.6
274.15	135.4	89.2	385.15	154.0	129.0
275.15	135.2	89.5	386.15	154.1	129.4
276.15	135.6	89.9	387.15	154.6	129.8
277.15	135.4	90.2	388.15	154.8	130.2
278.15	135.9	90.6	389.15	155.1	130.7
279.15	135.9	90.9	390.15	155.4	131.1
280.15	136.0	91.2	391.15	155.4	131.5
281.15	136.1	91.6	392.15	155.6	131.9
282.15	136.4	91.9	393.15	155.4	132.4
283.15	136.5	92.2	394.15	155.8	132.8
284.15	136.5	92.6	395.15	155.8	133.2
285.15	136.8	92.9	396.15	156.0	133.7
286.15	136.9	93.3	397.15	156.4	134.1
287.15	137.0	93.6	398.15	156.5	134.6
288.15	137.1	93.9	399.15	156.8	135.0
289.15	137.3	94.3	400.15	157.0	135.5
290.15	137.4	94.6	401.15	157.4	135.9
291.15	137.7	95.0	402.15	157.4	136.4
292.15	137.7	95.3	403.15	157.6	136.8
293.15	137.9	95.6	404.15	157.9	137.3
294.15	138.0	96.0	405.15	158.2	137.8
295.15	138.2	96.3	406.15	158.3	138.2
296.15	138.3	96.7	407.15	158.1	138.7
297.15	138.3	97.0	408.15	158.4	139.2
298.15	138.5	97.3	409.15	158.6	139.7
299.15	138.7	97.7	410.15	158.8	140.2
300.15	138.9	98.0	411.15	159.1	140.6
301.15	139.1	98.4	412.15	159.2	141.1
302.15	139.3	98.7	413.15	159.5	141.6
303.15	139.5	99.0	414.15	159.7	142.1
304.15	139.7	99.4	415.15	160.1	142.7
305.15	139.8	99.7	416.15	160.3	143.2

(*continued on next page*)

Table A.11 (*continued*).

Ethylene Carbonate, Liquid Phase and metastable liquid					
306.15	139.9	100.1	417.15	160.5	143.7
307.15	140.0	100.4	418.15	160.8	144.2
308.15	140.0	100.8	419.15	160.9	144.7
309.15	140.1	101.1	420.15	161.1	145.3
310.15	140.2	101.5	421.15	161.1	145.8
311.15	140.4	101.8	422.15	161.2	146.4
312.15	140.7	102.1	423.15	161.4	146.9
313.15	140.7	102.5	424.15	161.5	147.5
314.15	141.0	102.8	425.15	161.9	148.0
315.15	141.0	103.2	426.15	162.3	148.6
316.15	141.5	103.5	427.15	162.5	149.2
317.15	141.6	103.9	428.15	162.4	149.8
318.15	141.8	104.2	429.15	162.7	150.4
319.15	142.0	104.6	430.15	163.2	151.0
320.15	142.1	104.9	431.15	163.5	151.6
321.15	142.4	105.2	432.15	163.6	152.2
322.15	142.4	105.6	433.15	163.9	152.8
323.15	142.5	105.9	434.15	163.7	153.4
324.15	142.5	106.3	435.15	163.8	154.1
325.15	142.7	106.6	436.15	164.2	154.7
326.15	142.7	107.0	437.15	164.3	155.3
327.15	143.1	107.3	438.15	164.6	156.0
328.15	143.1	107.7	439.15	164.9	156.7
329.15	143.5	108.0	440.15	165.1	157.4
330.15	143.7	108.4	441.15	165.2	158.0
331.15	144.1	108.7	442.15	165.6	158.7
332.15	144.3	109.1	443.15	166.0	159.5
333.15	144.4	109.4	444.15	166.2	160.2
334.15	144.6	109.8	445.15	166.5	160.9
335.15	144.5	110.2	446.15	166.7	161.6
336.15	144.9	110.5	447.15	166.7	162.4
337.15	144.8	110.9	448.15	166.7	163.2
338.15	145.1	111.2	449.15	166.8	163.9
339.15	145.1	111.6	450.15	167.0	164.7
340.15	145.4	111.9	451.15	167.3	165.5
341.15	145.6	112.3	452.15	167.9	166.3
342.15	145.9	112.6	453.15	167.9	167.2
343.15	146.2	113.0	454.15	167.9	168.0
344.15	146.4	113.4	455.15	167.9	168.8
345.15	146.8	113.7	456.15	168.3	169.7
346.15	146.8	114.1	457.15	168.8	170.6
347.15	147.0	114.4	458.15	169.2	171.5
348.15	147.1	114.8	459.15	169.2	172.4
349.15	147.4	115.2	460.15	169.4	174.3
350.15	147.3	115.5	461.15	169.5	175.2
351.15	147.3	115.9	462.15	169.6	176.2
352.15	147.5	116.3	463.15	169.8	177.2
353.15	147.7	116.6	464.15	170.0	178.2
354.15	148.1	117.0	465.15	170.4	179.2
355.15	148.1	117.4	466.15	170.5	180.3
356.15	148.4	117.7	467.15	170.7	181.4
357.15	148.6	118.1	468.15	171.0	182.5
358.15	148.9	118.5	469.15	171.2	183.6
359.15	149.2	118.8	470.15	171.4	184.7
360.15	149.4	119.2	471.15	171.8	185.9
361.15	149.6	119.6	472.15	172.1	187.0
362.15	149.8	120.0	473.15	172.3	188.2
363.15	149.9	120.3	474.15	172.2	189.5
364.15	149.9	120.7	475.15	172.1	190.7
365.15	150.1	121.1	476.15	172.3	192.0
366.15	150.4	121.5	477.15	172.9	193.3
367.15	150.5	121.9	478.15	173.2	194.6
368.15	150.7	122.2	479.15	173.2	196.0
369.15	150.9	122.6	480.15	173.2	197.3
370.15	151.2	123.0	481.15	173.3	198.8
371.15	151.5	123.4	482.15	173.7	200.2
372.15	151.4	123.8	483.15	174.1	201.7
373.15	151.8	124.2	484.15	174.1	203.2
374.15	152.1	124.6	485.15	174.5	204.7
375.15	152.2	125.0	486.15	174.8	206.3
376.15	152.5	125.4	487.15	174.9	207.9
377.15	152.6	125.8	488.15	174.8	209.5
378.15	152.5	126.2	489.15	174.8	211.2
379.15	152.5	126.6	490.15	175.1	212.9

(*continued on next page*)

Table A.11 (*continued*).

Ethylene Carbonate, Liquid Phase and metastable liquid					
380.15	153.0	127.0	491.15	175.3	214.6
381.15	153.3	127.4	492.15	175.2	216.4
382.15	153.4	127.8	493.15	175.1	216.4
383.15	153.6	128.2			

[a] Standard uncertainty is $u(T)$ = 0.8 K, $u(p)$ = 0.1 p and the combined expanded uncertainty of the heat capacity is $U_c(C_{p,m})$ = 0.05 $C_{p,m}$ (0.95 level of confidence).

Certificate of Analysis

8.44011.0100 Ethylene carbonate for synthesis
Batch S7827611

	Batch Values	
Assay (GC, area%)	99.9	% (a/a)
Melting range (lower value)	35	°C
Melting range (upper value)	37	°C
Acid value	0.1	
Identity (IR)	passes test	

Due to its specific melting range the product may be solid, liquid, a solidified melt or a supercooled melt.

Date of examination (DD.MM.YYYY) 29.07.2019
Minimum shelf life (DD.MM.YYYY) 31.07.2024

Dr. Jörg Bauer
Responsible laboratory manager quality control

This document has been produced electronically and is valid without a signature.

Merck KGaA, Frankfurter Straße 250, 64293 Darmstadt (Germany): +49 6151 72-0
EMD Millipore Corporation - a subsidiary of Merck KGaA, Darmstadt, Germany
400 Summit Drive, Burlington, MA 01803, USA, Phone +1 (781) 533-6000
SALSA **Version 865042** /990000672017// Date: 29.07.2019

Page 1 of 1

Fig. A.11. Analysis certificate for ethyl carbonate.

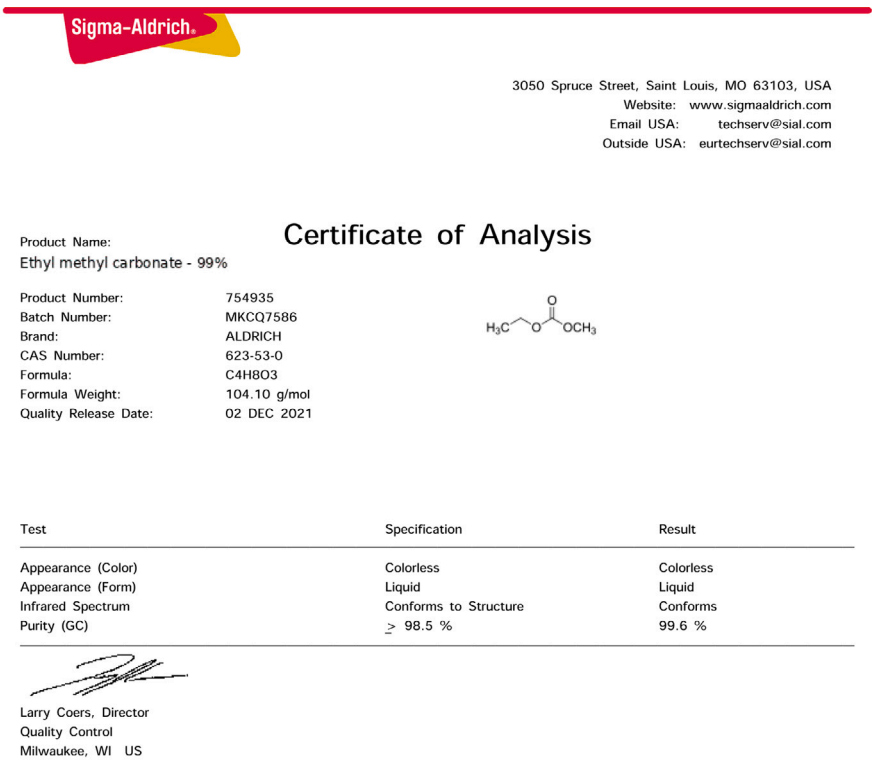

Sigma-Aldrich.

3050 Spruce Street, Saint Louis, MO 63103, USA
Website: www.sigmaaldrich.com
Email USA: techserv@sial.com
Outside USA: eurtechserv@sial.com

Certificate of Analysis

Product Name:
Ethyl methyl carbonate - 99%

Product Number:	754935
Batch Number:	MKCQ7586
Brand:	ALDRICH
CAS Number:	623-53-0
Formula:	C4H8O3
Formula Weight:	104.10 g/mol
Quality Release Date:	02 DEC 2021

Test	Specification	Result
Appearance (Color)	Colorless	Colorless
Appearance (Form)	Liquid	Liquid
Infrared Spectrum	Conforms to Structure	Conforms
Purity (GC)	≥ 98.5 %	99.6 %

Larry Coers, Director
Quality Control
Milwaukee, WI US

Sigma-Aldrich warrants, that at the time of the quality release or subsequent retest date this product conformed to the information contained in this publication. The current Specification sheet may be available at Sigma-Aldrich.com. For further inquiries, please contact Technical Service. Purchaser must determine the suitability of the product for its particular use. See reverse side of invoice or packing slip for additional terms and conditions of sale.

Version Number: 1 Page 1 of 1

Fig. A.12. Analysis certificate for ethyl methyl carbonate.

Data availability

Data will be made available on request.

References

[1] K.-H. Kim, D.-W. Kim, C.-W. Kim, J.-C. Koh, D.-W. Park, Synthesis of dimethyl carbonate from transesterification of ethylene carbonate with methanol using immobilized ionic liquid on commercial silica, Korean J. Chem. Eng. 27 (5) (2010) 1441–1445, http://dx.doi.org/10.1007/s11814-010-0229-0.

[2] J.-C. Lee, M.H. Litt, Ring-opening polymerization of ethylene carbonate and depolymerization of poly(ethylene oxide- co-ethylene carbonate), Macromolecules 33 (5) (2000) 1618–1627, http://dx.doi.org/10.1021/ma9914321.

[3] R.C. Shurtz, J.C. Hewson, Review—Materials science predictions of thermal runaway in layered metal-oxide cathodes: A review of thermodynamics, J. Electrochem. Soc. 167 (9) (2020) 090543, http://dx.doi.org/10.1149/1945-7111/ab8fd9.

[4] W.-C. Chen, Y.-W. Wang, C.-M. Shu, Adiabatic calorimetry test of the reaction kinetics and self-heating model for 18650 Li-ion cells in various states of charge, J. Power Sources 318 (2016) 200–209, http://dx.doi.org/10.1016/j.jpowsour.2016.04.001.

[5] P.J. Bugryniec, J.N. Davidson, S.F. Brown, Computational modelling of thermal runaway propagation potential in lithium iron phosphate battery packs, Energy Rep. 6 (2020) 189–197, http://dx.doi.org/10.1016/j.egyr.2020.03.024.

[6] A.M. Domingues, R.G. De Souza, Review of life cycle assessment on lithium-ion batteries (LIBs) recycling, Next Sustain. 3 (2024) 100032, http://dx.doi.org/10.1016/j.nxsust.2024.100032.

[7] I. Vasil'ev, A. Korkhov, The heat capacities and enthalpies of fusion and the thermodynamic properties of solid and liquid ethylene carbonate, Zh. Fiz. Khim. (1973) 2710.

[8] M.S. Ding, Liquid solid phase equilibria and thermodynamic modeling for binary organic carbonates, J. Chem. Eng. Data 49 (2) (2004) 276–282, http://dx.doi.org/10.1021/je034134e.

[9] Y. Chernyak, J.H. Clements, Vapor pressure and liquid heat capacity of alkylene carbonates, J. Chem. Eng. Data 49 (5) (2004) 1180–1184, http://dx.doi.org/10.1021/je034173q.

[10] W.J. Peppel, Preparation and properties of the alkylene carbonates, Ind. Eng. Chem. 50 (5) (1958) 767–770, http://dx.doi.org/10.1021/ie50581a030.

[11] L. Vogdanis, B. Martens, H. Uchtmann, F. Hensel, W. Heitz, Synthetic and thermodynamic investigations in the polymerization of ethylene carbonate, Die Makromol. Chem. 191 (3) (1990) 465–472, http://dx.doi.org/10.1002/macp.1990.021910301.

[12] V. Pokorný, V. Štejfa, M. Fulem, C. Červinka, K. Růžička, Vapor pressures and thermophysical properties of ethylene carbonate, propylene carbonate, γ-valerolactone, and γ-butyrolactone, J. Chem. Eng. Data 62 (12) (2017) 4174–4186, http://dx.doi.org/10.1021/acs.jced.7b00578.

[13] Q. Wang, J. Sun, X. Yao, C. Chen, Micro calorimeter study on the thermal stability of lithium-ion battery electrolytes, J. Loss Prev. Process. Ind. 19 (6) (2006) 561–569, http://dx.doi.org/10.1016/j.jlp.2006.02.002.

[14] G. Höhne, W. Hemminger, H.-J. Flammersheim, Differential Scanning Calorimetry, second ed., Springer Berlin, Berlin, 2010.

[15] G. Della Gatta, M.J. Richardson, S.M. Sarge, S. Stølen, Standards, calibration, and guidelines in microcalorimetry. Part 2. Calibration standards for differential scanning calorimetry* (IUPAC technical report), Pure Appl. Chem. 78 (7) (2006) 1455–1476, http://dx.doi.org/10.1351/pac200678071455.

[16] X. Zhang, J. Zuo, C. Jian, Experimental isobaric vapor liquid equilibrium for binary systems of ethyl methyl carbonate methanol, ethanol, dimethyl carbonate, or diethyl carbonate at 101.3 kPa, J. Chem. Eng. Data 55 (2010) 4896–4902, http://dx.doi.org/10.1021/je100494z.

[17] A. Shimkin, Optimization of DSC calibration procedure, Thermochim. Acta 566 (2013) 71–76, http://dx.doi.org/10.1016/j.tca.2013.04.039.

[18] V.A. Drebushchak, Calibration coefficient of a heat-flow DSC; Part II. Optimal calibration procedure, J. Therm. Anal. Calorim. 79 (1) (2005) 213–218, http://dx.doi.org/10.1007/s10973-004-0586-1.

[19] R. Seyler, Parameters affecting the determination of vapor pressure by differential thermal methods, Thermochim. Acta 17 (2) (1976) 129–136, http://dx.doi.org/10.1016/0040-6031(76)85019-8.

[20] R. Páramo, M. Zouine, C. Casanova, New batch cells adapted to measure saturated heat capacities of liquids, J. Chem. Eng. Data 47 (2002) 441–448, http://dx.doi.org/10.1021/je0155103.

[21] M.S. Ding, T.R. Jow, Properties of PC-EA solvent and its solution of LiBOB comparison of linear esters to linear carbonates for use in lithium batteries, J. Electrochem. Soc. 152 (6) (2005) A1199, http://dx.doi.org/10.1149/1.1914757.

[22] F. Baakes, M. Lüthe, M. Gerasimov, V. Laue, F. Röder, P. Balbuena, U. Krewer, Unveiling the interaction of reactions and phase transition during thermal abuse of Li-ion batteries, J. Power Sources 522 (2022) 230881, http://dx.doi.org/10.1016/j.jpowsour.2021.230881.